APP Template V1.70 Article id: ppcfaafbbf Typesetter: MPS Date received by MPS: 17/01/2019 PE: CE: LE:

IOP Publishing Plasma Physics and Controlled Fusion

Plasma Phys. Control. Fusion **00** (2019) 000000 (12pp)

Current sheets in planetary magnetospheres

Lev Zelenyi[1], Helmi Malova[2,1], Elena Grigorenko[1], Victor Popov[1,3,4] and Dominique Delcourt[5]

[1] Space Research Institute of the Russian Academy of Sciences, Moscow, Russia
[2] Scobeltsyn Institute of Nuclear Physics, Lomonosov Moscow State University, Moscow, Russia
[3] Physics Faculty of Lomonosov Moscow State University, Moscow, Russia
[4] National Research University 'Higher School of Economics', Moscow, Russia
[5] CNRS, Universite d'Orleans–CNES, ~~Orlean~~, France

E-mail: lzelenyi@iki.rssi.ru

Received 15 October 2018, revised 29 November 2018
Accepted for publication 3 January 2019
Published DD MM 2019

Abstract

In this article we aim to highlight the problems related to the structure and stability of the comparatively thin current sheets that were relatively recently discovered by space missions in the magnetospheres of the Earth and planets, as well as in the solar wind. These magnetoplasma structures are universal in collisionless cosmic plasmas and can play a key role in the processes of storage and release of energy in the space environment. The development of a self-consistent theory for these sheets in the Earth's magnetosphere, where they were first discovered, has a long and dramatic history. Solution of the problem of the thin current sheet structure and stability become possible in the framework of a kinetic quasi-adiabatic approach required to explain their embedding and metastability properties. It was found that the structure and stability of current structures are completely determined by the nonlinear dynamics of plasma particles. Theoretical models have been developed to predict many properties of these structures and interpret many experimental observations in planetary magnetospheres and the heliosphere.

Keywords: space plasma, current sheet, energy storage and release, instability

SQ1 (Some figures may appear in colour only in the online journal)

1. Peculiarities of planetary magnetospheres as a result of solar wind–magnetic field interactions

Q1 After satellite measurements in the 1960s and 1970s it became evident that the Earth's dipole magnetic field actively interacts with the solar wind (SW) [1–4] producing the streamlined flow of the solar plasma with the frozen-in interplanetary magnetic field (IMF). This interaction leads to the formation of the giant magnetic cavity (magnetosphere) surrounding a planet, where the SW plasma is deflected by the intrinsic (or induced, for some planets) magnetic field. On the basis of the experimental observations available at the time, Ness [5] described the Earth's magnetosphere as a non-spherical object resembling a very compressed dipole at the dayside and as a non-dipole shaped magnetic structure resembling a cometary tail at the Earth's nightside (see figure 1). This structure, strongly stretched by the SW at the nightside was named the magnetotail. The Earth's magnetotail seemed to be a very elongated structure, about $250R_E$ to $300R_E$ ($R_E \approx 6400$ km is the radius of the Earth). Electric currents of about 10^6 A flow in its symmetry plane in the direction from dawn to dusk. This current sheet (CS) self-consistently supports the oppositely directed magnetic fields in a vast region named the 'magnetotail lobes'. The magnetotail has a tendency to flare downstream from the Earth, forming approximately the surface of a rotational paraboloid [6]. Observations showed that the thickness of the magnetotail CS depends on the state of the magnetosphere [7–9]: in the growth phase of substorms (global magnetic perturbations) the magnetotail CS is thinned from about several R_E to a thickness of about one to several proton gyroradii, i.e. about 250–4000 km [7–11]. It is supposed that this extremely thin current sheet (TCS) in the Earth's magnetotail plays a key role in the development of a substorm cycle of magnetic energy 'storage–release'. CS processes can trigger the switching of the evolutionary dynamics of energy storage in the magnetotail to the explosive-like release of the stored energy due to instability, which can even completely disrupt

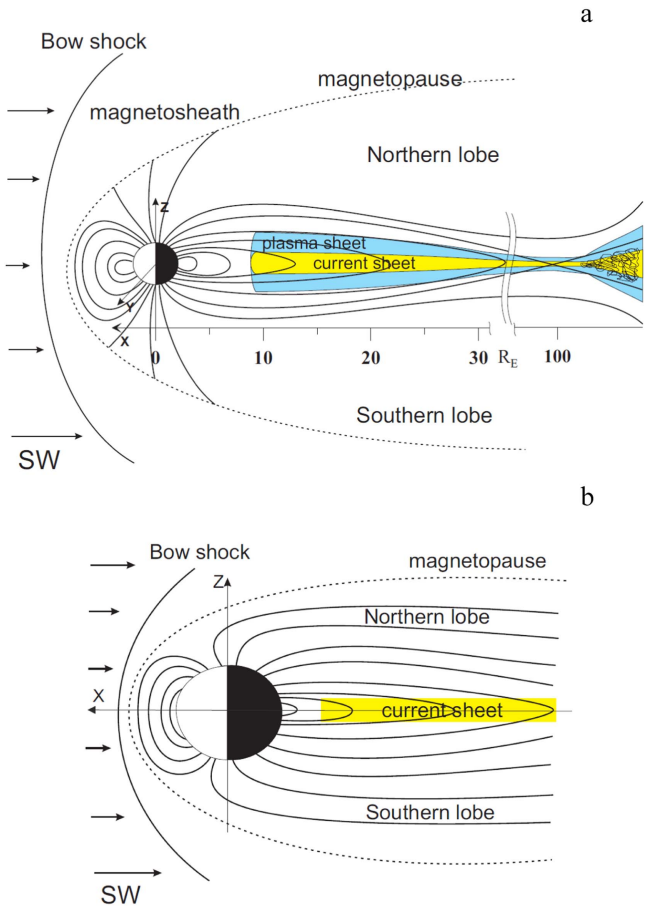

Figure 1. Scheme of the magnetospheres of Earth (a) and Mercury (b) (adapted from [15]); here black lines are magnetic field lines; colored areas correspond to charged particle trajectories near the planet.

the CS itself [11, 12]. Moreover, natural turbulence in TCSs is also responsible for the energization of the magnetospheric plasma, particularly for plasma heating, acceleration and transport in the magnetosphere.

Due to numerous modern spacecraft missions it is now clear that TCSs can be observed everywhere in space plasmas. They seem to be a universal structures in space plasmas responsible for energy storage and release, magnetic reconnection, plasma acceleration and other important processes in all planetary magnetospheres, in the SW [11, 13–16], the solar corona [17] and in many laboratory experiments [18].

Planetary magnetospheres are really the result of the interaction of supersonic SW flows with the intrinsic magnetic fields of planets or their conducting ionospheres. In this sense one can see the universality of both magnetospheric-type interactions and the scaling factor characterizing their spatial and temporal characteristics compared with that of the Earth. One can distinguish the general basic properties of planetary magnetospheres. First, they can have an intrinsic source of the magnetic field due to internal dynamo processes (Mercury, Earth, giant and ice planets). Second they can have an induced magnetosphere (Venus and Mars) and at the same time entirely lost or weak residual magnetic fields. Relatively small planets with a weaker magnetic field, like Mercury, might have a magnetosphere with a much simpler structure than the larger complicated magnetospheres of Earth and the giant planets. Third, the majority of magnetospheric magnetotail CSs have a flat configuration in the equatorial plane [19]. An axisymmetric cylindrical current configuration is characteristic for planets which have a pole-on position of their magnetic dipoles relative to the direction of flow of the SW (e.g. Uranus, Neptune and the dwarf planet Pluto) [20–22].

For fast rotating giant planets with a strong intrinsic magnetic field the process of corotation (generation of an electric field due to planetary rotation which involves the plasma surrounding the planet to (co-)rotating with the same angular velocity) and the presence of small satellites as strong source of plasma besides the SW could play a significant role in the formation of specific magnetodisk configurations with a strong ring electric current about (90–160) $\times$ 10^6 A [23, 24]. The fine structure of the magnetodisk current in the equatorial plane of the planet cannot be described fully in a framework of a magnetohydrodynamics (MHD) approach [25, 26] because of the small transverse disk thickness. This magnetodisk current can be also a kind of cylindrically shaped TCS that could be considered as a tangential discontinuity in a MHD consideration.

Below we elucidate some aspects of the structure and stability of planetary magnetospheres in relation to the key universal structures within them, i.e. TCSs playing an important role in the general energy circulation within them [16]. We will consider planets with plane current systems, as these have been much more fully investigated compared with distant planets that have either quasi-steady or intermittent cylindrical shapes depending on the tilt angle of their dipole moments relative to the flow of the SW.

2. Magnetospheres of planets: common features and differences

A comparison of two Earth-type magnetospheric configurations is shown in figure 1. Hereafter we will use the standard Geocentric Solar Magnetospheric System, where the *X*-axis is directed from the center of the Earth to the center of the Sun, the *Z*- axis coincides with the direction of the Earth's dipole and the *Y*-axis is directed correspondingly from the dawn side to dusk side. Q2

Streamlining of magnetic dipoles by a supersonic SW can lead to the formation of a bow shock [27] (a standing wave upstream of the magnetosphere), as displayed in figure 1 for both planets. The Earth's magnetopause is the very narrow current region with a thickness of about 100–1600 km (see, e.g., [28] and references therein) which separates the magnetosphere itself from the SW. In these vast regions a TCS with a magnetic field reversed in a neutral plane can be revealed. The transitional region between the bow shock and magnetopause is the magnetosheath, where plasma motion is strongly turbulent. The shape of the magnetopause is determined by the balance between the

dynamical pressure of the SW and the static magnetic pressure of the planetary magnetic field [29].

The inner magnetosphere contains radiation belts, representing the regions in the dipole magnetic field with relatively stable trapping of charged particles with energies from about 100 keV to several hundred MeV. The polar auroral oval is the prominent current system that appears at the boundary between the closed and open magnetic field lines [30]. Figure 1 demonstrates the stretched magnetic configuration, named a magnetotail, at the nightside of both planets [5, 31]. A typical plasma density for Earth is 0.3–0.5 ions/cm^3 and typical proton energies are of the order of several keV; electron energies are usually five to eight times lower. Large-scale electric current flows from the dawn side to the dusk side and close over the magnetopause [11]. A CS in the neutral plane can stably support this stretched magnetic configuration with a tangential component reversing its sign in the neutral plane [32]. At a distance $X \sim -100R_{\rm E}$ magnetic field lines of the magnetospheric dipole, convecting in the direction of flow of the SW, can be reconnected at the distant magnetic X-line and move back, backwards, to the Earth; separated IMF magnetic lines move downstream in the tailward direction (figure 1(a)). The earthward convective flow stops at a distance of about $7R_{\rm E}$ to $9R_E$ and then plasma flow moves around the Earth, forming a close ring current. Sometimes it is considered that there is a further external radiation belt of the Earth along with the abovementioned internal ones. It should be noted that TCSs are usually observed near X-lines in the magnetotail and lie on both their sides. Thus a magnetotail can play the role of an energy reservoir where an excess of free magnetic energy gained during substorms might be accumulated in the TCS formed in a neutral plane, and can then be quickly released in a form of kinetic energy of plasma flows near newly formed reconnection regions. This theoretical concept is now rather convincingly supported by experimental observations [11].

Planetary magnetospheres might be quite different in their dimensions but all of them have a similar topology. Therefore one can suppose that self-similar scaling laws could be applied for their comparison. Taking into account that the density of the SW decreases as an inverse square of the distance r from the Sun, one can estimate the relative stand-off SW distance [33]:

$$\frac{D_{\rm p}}{D_{\rm E}} = \left(\frac{r_{\rm p} M_{\rm p}}{M_{\rm E}}\right)^{1/3}. \qquad (1)$$

Here, $D_{\rm p}$, $D_{\rm E}$, $M_{\rm p}$ and $M_{\rm E}$ are, respectively, the subsolar radii and dipole moments of planetary magnetospheres (p) and the Earth (E), $r_{\rm p}$ is the heliocentric distance of the planet in astronomical units AU (1 AU being the distance from the Earth to the Sun). This scaling factor (1) has a universal character in the hierarchy of magnetospheric scales and might also be applied to estimate other spatial and temporal characteristics of magnetospheres of different planets and to compare results with available observations.

Now let us consider the peculiarities of the magnetosphere of Mercury (figure 1(b)), the second planet of Earth's type. It was a great surprise to scientists that this small iron planet with radius of 2400 km possesses an intrinsic magnetic field [24]. Mariner 10 flybys near Mercury in 1974 and 1975 demonstrated that the size of its magnetosphere is about 5% of that of the Earth. The spatial scales of Mercury's magnetosphere, accordingly to scaling law (1) might be estimated relative to the Earth's spatial distances by a factor of about 8 [34]. Thus the weak magnetic field of Mercury stops the flow of the SW at a distance of about $0.6R_{\rm M}$ ($R_{\rm M}$ being the radius of Mercury) from the surface of the planet. Thus Mercury occupies the major part of its magnetosphere; as a result it has no ionosphere, no radiation belts and no ring current [35]. Mercury's magnetotail is observed at distance up to $10R_M$ at the nightside. Observations by Mariner 10 have shown that the relatively thick lobes of Mercury's magnetosphere are separated by a very thin CS with a thickness of about 150–300 km [36], which is comparable with the gyroradii of protons. Particle motion, as well as particle transfer and acceleration in the magnetotail, is strongly non-adiabatic and can be described in a framework of a quasi-adiabatic approach (see [11, 16] and references therein). Generally, due to its proximity to the Sun and its small size, the Hermean magnetosphere is strongly driven by the SW. Substorms here can occur almost every minute [37].

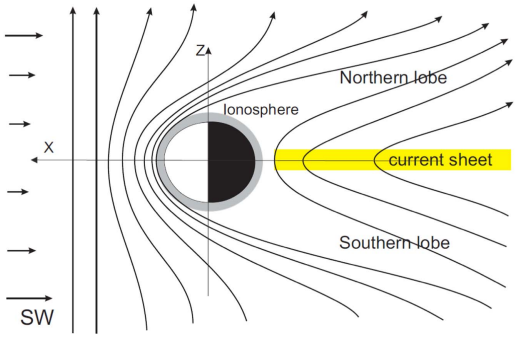

Figure 2. The concept of an induced magnetosphere. The planet is surrounded by an ionosphere which supports the induced magnetic field with an elongated magnetotail-like structure in the downstream direction. The ionosphere separates the planetary plasma from the SW. Supersonic flow of the SW produces a bow shock upstream of the planetary ionosphere representing the conducting obstacle.

In contrast to the Earth and Mercury, which have intrinsic magnetic fields, the planetary fields of Venus and Mars, schematically shown in figure 2, are not able to substantially deflect the SW. The nature of the interaction between the SW and non-magnetized objects depends on the electrical conductivity of the body. The incident plasma stream could be slowed and then deflected by the induced magnetic field if a current loop going over the conducting planetary surface and/or its conducting ionosphere to the SW is formed in the planet's plasma environment [35]. As a result, a magnetosphere-like cavity, named the 'induced magnetosphere', with an elongated magnetotail could be formed around the planet (figure 2). Thus Mars and Venus do not have large-scale intrinsic magnetic fields but have ionospheres that provide the conducting paths to close the induced currents and generate such an exotic 'magnetosphere'. There is no distinct boundary

like the Earth's magnetopause. The ionopause plays the role of a 'barrier' separating the planetary plasma from the plasma of the SW. The system of shielding induced currents is modified by a comet-like pickup process engaging exospheric and ionospheric ions [38, 39]. The general processes there are: (1) photoionization of planetary atoms; (2) mass loading of the SW flow by planetary ions; (3) differential draping of magnetic field lines; and (4) formation of a magnetotail from the field lines bent due to the differential mass loading. These processes play a key role in formation of the induced magnetosphere by IMF field lines convecting around the planet.

Global magnetic perturbations are characteristic of the induced magnetospheres of Mars and Venus, depending on their interaction with the SW plasma flow. It was shown that analogous to the Earth's magnetic storms significant magnetic activity also takes place at Mars [40]. Martian magnetic storms are found to be associated with passage of the planet across the heliospheric CS, accompanied by changes in IMF polarity. Mars Express measurements have shown that during Martian magnetic storms strong perturbations occur in the magnetosphere and ionosphere. The magnetic barrier formed by the pile-up of IMF in front of the ionopause decays and does not provide any shielding from the incoming SW. Large blobs (clouds) of SW plasma might penetrate to the Martian magnetosphere and extinguish the dense plasma from the ionosphere. The topside region of the ionosphere becomes very fragmented and consists of intermittent cold/low energized plasmas [41].

A quantitative model of the Venusian magnetosphere was developed by Vaisberg and Zelenyi [42] who followed the dynamics of interplanetary magnetic field lines loaded by heavy ions picked up by the planet. While central parts of the field lines flowing through the Venusian exosphere are mass loaded and decelerated, their ends immersed into the SW flow are moving with unperturbed SW velocity. This results in strong bending of the interplanetary magnetic field lines and formation of a field reversal region at the nightside resembling the magnetotail. Such a tail is formed from open mass-loaded field lines and is named the 'accretion magnetotail'.

The magnetotail of the induced magnetosphere of Venus was investigated by the Venus Express spacecraft. It was shown that the magnetic field of Venus is quite dynamic, indicating that reconnection processes can also take place in the magnetotail. This could explain the presence of energized ions with energies from 1500 to 2000 eV. Nevertheless sometimes magnetotail magnetic measurements revealed a very quiet tail with a TCS in the central part populated only by low-energy ions [43, 44].

Due to successful missions by Pioneers 10 and 11, Voyagers 1 and 2 and the Galileo spacecraft the basic properties of the Jovian and Saturnian magnetospheres are known in general. Jupiter is the largest planet of the Solar System (radius $R_J \approx 71\,400$ km); it has the strongest magnetic field with a magnetic moment 18 000 times larger than that of the Earth. The Jovian magnetotail extends in the antisunward direction to 650×10^6 km reaching the orbit of Saturn [35]. The structure of this magnetosphere is more complex than that of the Earth (see figure 1(a)), containing a bow shock,

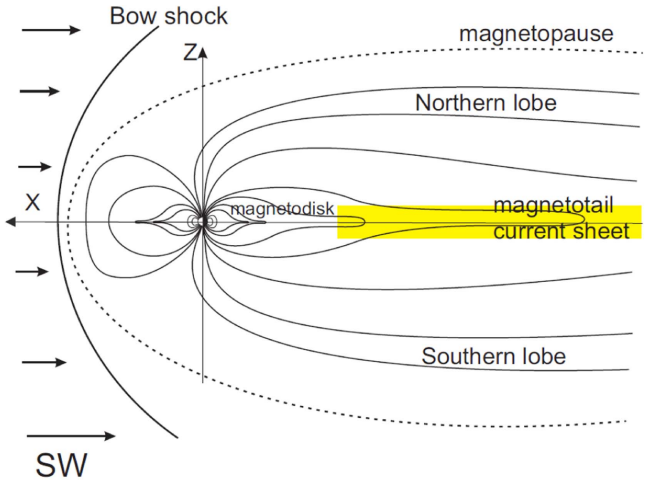

Figure 3. Schematic view of the structure of the Jovian magnetosphere.

magnetopause, magnetotail and magnetodisk (figure 3). The Jovian bow shock is located at an average distance about 7×10^6 km from the center of the planet; the magnetopause is observed at a distance of about $60R_J$ to $70R_J$.

Because of the additional amount of plasma from the Jovian satellite Io, known for its volcanic activity, the size of the Jovian magnetosphere is substantially expanded, giving an additional component to the balancing of pressure against the pressure of the SW. At the nightside of the planet, the magnetosphere of Jupiter is stretched into a long magnetotail similar to that of the Earth; two lobes are separated by a TCS in the center. The magnetotail CS is closed on the magnetopause due to Chapman–Ferraro currents.

It was proposed in [45] that steady-state reconnection at the external edges of the Jovian magnetodisk should support the formation of plasmoids and the return of empty flux tubes to the inner magnetosphere.

Galileo observations indicated that beyond $40R_J$ the Jovian magnetodisk CS is disrupted and beyond $50R_J$ at the nightside tail the magnetic field could be explosively reconnected [44]. These disruption events are not regular; they have characteristic time scales from 4 h (for small events) to about 24 h (for large events). Because of these reconnection processes plasmoids enter into the Jovian tail and provoke fast reconnection in the magnetotail CS at the nightside of the planet. This could support the close plasma and magnetic flux circulation around the planet. These plasma disturbances could be interpreted as Jovian substorms. Therefore, unlike for the Earth-like planets, the Jovian substorms depend substantially on internal convection and are only slightly driven by SW–magnetosphere interaction.

Summing up this section, one can say that the magnetosphere of the planets which have or do not have an intrinsic magnetic field have differences but also many similarities. The magnitude of the planetary magnetic dipole field interacting with the supersonic SW flow determines the scaling factor (see equation (1)) describing the hierarchy of magnetospheric scales relative to that of the Earth. In turn, the sizes of the magnetospheres determine their relationship to driving

by the SW. The larger the magnetosphere (e.g. Jupiter), the less the magnetospheric structures and processes are driven by the SW. The smaller the magnetosphere (e.g. Mercury, Earth), the more it depends on transient SW flows. Magnetospheres are shielded from the SW by a complicated system of currents flowing along their boundary structures (bow shocks, magnetopauses, magnetotails). TCSs seem to be universal structures characteristic of all magnetospheres where the storage and release of energy takes place as a result of global perturbations, storms and substorms. Below we consider in more detail the properties of CSs in planetary magnetotails and their consequences for the planetary environments and energy balance.

3. Experimental observations of multiscale current sheets as universal structures in space plasma

Spacecraft data obtained in the Earth's magnetosphere by Geotail, Interball, Cluster and other spacecraft have provided an unprecedented opportunity to gain new knowledge and develop a new generation of models to investigate CSs in the magnetosphere. In recent years the attention of many researchers has been focused on extremely thin CSs with thicknesses of about an ion Larmor radius or less which were observed in the magnetotail at different distances from the Earth [7–10]. The region at the near-Earth edge of the magnetotail CS is of particular interest, because, first of all, it is more easily accessible by spacecraft and secondly it is the presumed domain of substorm initiation, explosive-like evolution and energy transformations. TCSs in this region may appear as a result of enhanced plasma convection in the course of the substorm growth phase and, as we have mentioned above, might play a role of the reservoir of magnetic energy, which could be released after disruption of the CS at the onset of the substorm expansion phase.

The structure and properties of TCSs in the Earth's magnetosphere have now been investigated by many spacecraft-borne '*in situ*' experiments, including recent multipoint Cluster measurements [10]. The essential properties of TCSs are different from those of CSs which are observed under quiet conditions in the magnetosphere. Satellite investigations have revealed the following particular properties of TCSs:

(1) A very small thickness $L \sim \rho_p \sim 250$–1000 km, where ρ_p is the proton gyroradius. Such thin current profiles are often observed in the Earth's magnetosphere [7–12, 29, 43]. Figure 4 demonstrates a characteristic crossing of the cross-tail CS in the Martian magnetotail from the catalog of intervals published in [46]. Here one can clearly see that the current density profile has a multiscale embedded character: an extremely thin CS (with a thickness of less than 100 km) is embedded inside a thicker sheet with a thickness of about 300 km. Analogous CS intersections have been shown by the Venus Express in the Venusian magnetotail [47] and by Mariner 10 for Mercury [48]. In the latter case the time scale of CS crossing was 40 s and the jump of the magnetic field was 80 nT. The thickness of the CS observed, probably, after dipolarization was estimated as 150 km. For comparison, the gyroradius of a proton with an energy of 2 keV is about 1000 km in a magnetic field with a magnitude of 40 nT.

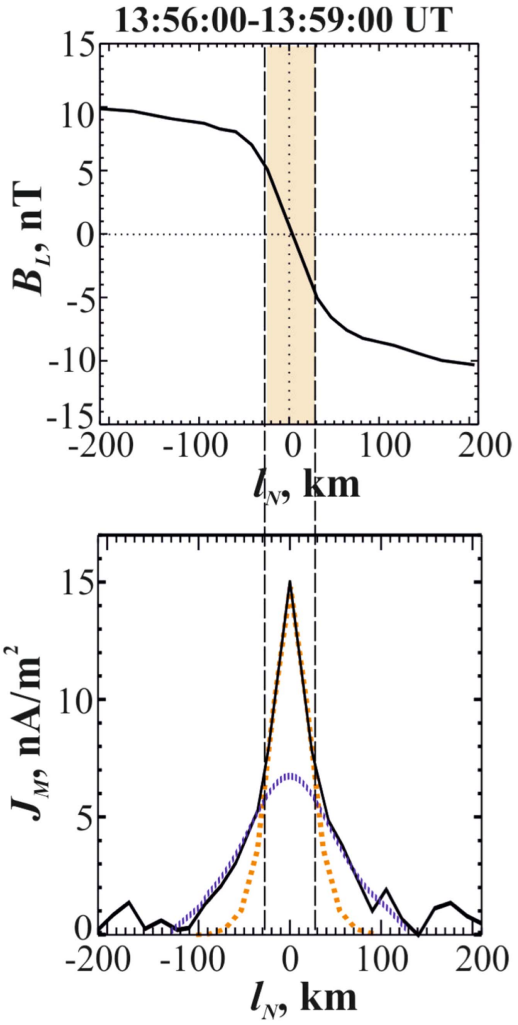

Figure 4. An example of the characteristic spatial profiles of magnetic field (B_L) and electric current density (J_m) observed in the Martian magnetotail on 7 December 2016 at 13:56–13:59 UT.

(2) A large current density, which might be 10–20 times larger than that under usual tail conditions ($\sim$10 nA m^{-2} for the Earth).

(3) A very stretched shape of the magnetic field lines, with $B_z/B_x \sim 0.1$.

(4) Ions in open (so-called Speiser) orbits are usually the main current carriers across the sheet [11, 16]. Electron currents can dominate in the narrow region in the neutral plane and are presumably produced by drift currents [49].

(5) The current density profile does not usually coincide with the plasma density profile: a TCS is embedded within a thicker plasma sheet [11, 16]. It is shown on the basis of ISEE 1 and ISEE2 observations in the Earth's magnetosphere that TCSs with thicknesses of about $0.2R_E$ were found to be embedded into a much

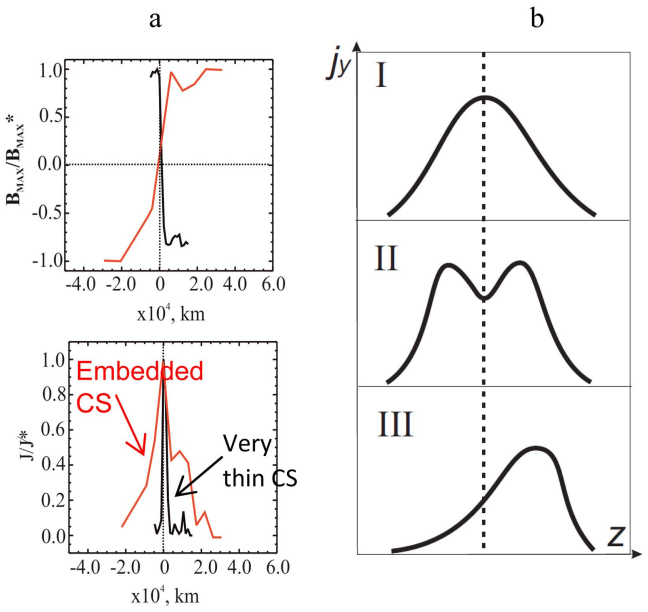

Figure 5. Different kinds of TCS in the space plasma: (a) embedded strong CSs in the SW observed within the heliospheric plasma sheet (adapted from [14]); (b) average vertical profiles in the Earth's magnetotail for center peaked (I), bifurcated (II) and asymmetrical CSs (III) (adapted from [50]).

broader plasma sheet with a transverse scale L of about $3R_E$ to $4R_E$. A multiscale character of multiple TCSs in the region of the heliospheric plasma sheet in the SW was suggested by Stereo-A observations [14], shown in figure 5(a).

(6) Cluster data [50] showed that TCS can not only have a classical bell-shaped current profile (figure 5(b), I) but that these profiles could be bifurcated, with two maxima of current density at the edges and minima in the center (see figure 5(b), II).

(7) In some observations one can see unusual sheets with current peaks shifted from zero of the magnetic field and having an asymmetrically shaped current density (figure 5(b), III). The reasons for this asymmetry have been studied (e.g. [51, 52]).

(8) TCSs are metastable, i.e. after their formation they remain stable during the entire growth phase of substorms (time periods in the Earth's magnetotail from 15 min to 2 h) and after this they can be explosively destroyed in the course of the substorm expansion phase, resulting in particle thermalization and acceleration as well as significant enhancement of wave activity [10, 11, 13, 46, 53].

4. TCSs as reservoirs of magnetic energy

The idea that solar flares are the result of the release of energy due to disruption of CSs was developed by Syrovatsky [17]. Accumulated magnetic energy can be transformed in solar flares to both the thermal and bulk energy of particle motion. Now it is known that magnetic reconnection in TCSs formed due to crossing of magnetic loops is responsible for solar flares in solar corona. Generally TCSs in the heliospheric and magnetospheric plasma are the places of transformation of stored magnetic energy into kinetic energy of plasma particles, their transport and acceleration. Because a TCS separates two regions with oppositely directed magnetic field lines, their reconnection usually leads to CS disruption and corresponding sheet filamentation [53].

The collisionless tearing (current filamentation) instability is the most probable mechanism initiating the beginning of magnetic reconnection in a TCS, consequent plasma acceleration and plasmoid formation. Theoretical analysis in [54] showed that a Harris-like CS [55] with only one tangential magnetic component B_x is always unstable for the tearing mode. But later it was shown [56] that the effect of electron compressibility prevents the development of a tearing mode in a model of a Harris-like CS with a small normal magnetic field component (this a small B_z component is always unavoidably persistent in planetary magnetotails). A sufficiently strong electrostatic field appears to support charge neutrality of the perturbed system because electrons (unlike ions) are magnetized by the B_z field. Thus the energy of perturbed electrons exceeds the available free energy of the CS, preventing the development of a tearing mode [57].

The problem of full stability of the collisionless tearing mode in a CS with non-zero normal magnetic component was a theoretical mystery for several decades. Many efforts were made to make models of an unstable magnetotail configuration taking into account, for example, kink and other modes (see, e.g., [11, 13, 58–60] and references therein). It has been shown in these studies that all these instabilities either develop very slowly or saturate at a very low level. All these early studies of tearing modes were based on CS models with a non-zero normal component assuming at the same time isotropic distribution functions of the plasma components. None of the attempts to expand the instability region considering the mechanisms of plasma microturbulence, chaotic scattering, bending and coupling with other modes like ballooning [11, 13] were successful. Multipoint observations of the spacecraft missions in the tail of Earth's magnetosphere, and later in other planetary magnetospheres and in the SW, reignited interest in the stability of CSs, since these observations confirmed that the CSs discussed in early papers by Syrovatskii [17] can be observed not only in planetary magnetospheres but also in the SW and solar corona. In [62] a solution to this paradox of full stability of a Harris CS with B_z was outlined and the tearing stability of a more suitable and realistic quasi-adiabatic model was investigated. In particular, the most important property of metastability was explained in the framework of this model. Later other kinds of unstable modes (king, sausage, oblique tearing, drift, etc.) were investigated [63]. Below we present a quasi-adiabatic model of a TCS which can explain the observed features of TCS structure and dynamics.

5. Quasi-adiabatic motion and equilibrium CS models

In the simplest one-dimensional (1D) collisionless CS model (Harris 1959) the shifted Maxwellian distributions for both ions and electrons were considered:

$$f_\alpha(v) = n_\alpha(z)\left(\frac{m_\alpha}{2\pi T_\alpha}\right)^{3/2} \times \exp\left\{-m_\alpha \frac{(v_x^2 + (v_y - V_{\alpha y})^2 + v_z^2)}{2T_\alpha}\right\},$$
$$n_\alpha(z) = n_0 \exp(e_\alpha V_{\alpha y} A_y(z)/cT_\alpha),$$
$$\frac{dB_x}{dz} = \frac{4\pi}{c}\sum_{\alpha=i,e}\int e\vec{v} f_\alpha(\vec{v}, z)d\vec{v}, \sum_{\alpha=i,e} e_\alpha n_\alpha = 0, \varphi(z) = 0, \quad (2)$$

where T_α is the temperature of the $\alpha = i, e$ particles, m_α is the mass, $V_{\alpha y}$ is the flow velocity, $W_0 = m_\alpha v^2/2$ is the total particle energy and $P_y = m_\alpha v_y + (e/c)A_y(z)$ is the generalized momentum. Corresponding self-consistent profiles of current, magnetic field and plasma density have the form

$$B_x(z) = B_0 \tanh(z/L), \; n(z) = n_0/\cosh^2(z/L),$$
$$j_y(z) = J_0/\cosh^2(z/L)$$

where the half-thickness of the CS is equal to $L = 2(T_i + T_e)/\{cB_0(V_{iy} - V_{ey})\}$. The characteristic property of such a CS is that the profiles of current and plasma density coincide, because their transverse scale is the same.

The first 2D model of magnetotail CS was proposed in [64] to describe a relatively thick magnetotail CS with fully magnetized plasma particles. The general approach that was applied was the MHD approximation where the corresponding tensor of plasma pressure is assumed to be isotropic. In such models the tension of the magnetic field lines is balanced by the gradient of plasma pressure in the Earth–Sun direction. The semifluid approach supposes CS anisotropy with a diagonal pressure tensor [65]. None of these models can be applied within TCSs where guiding center approximation is violated.

A pioneering analysis of particle dynamics in the neutral plane with strong transverse magnetic gradients was published by Speiser [64]. It was shown that in such CSs protons are demagnetized in the neutral plane, but their quasi-adiabatic integral of transverse (along the z coordinate) oscillations $I_z = (1/2\pi)\oint p_z dz$ is approximately conserved. This kind of particle motion was later called quasi-adiabatic [66]. Unlike protons in TCSs, electrons are fully magnetized, therefore the dynamics of different plasma particle species is drastically different. The models of an extremely thin CS with Speiser's ions as the main current carriers were developed later in [49, 67, 68]. In [49] it was demonstrated that electrons can be current carriers together with quasi-adiabatic protons due to strong gradient drift currents, but they sensitively depend on the curvature of magnetic field lines related to the value of the normal magnetic component. This new type of extremely thin plasma equilibrium with thickness $L \sim \rho_L$ (where ρ_L is the ion gyroradius) could not be supported by longitudinal pressure gradients but only by the off-diagonal terms of the pressure tensor. It was shown that these 1D magnetic configurations are almost homogeneous along the Earth–Sun direction [69]. Unlike in isotropic models of relatively thick CSs (both MHD and kinetic ones), plasma pressure in TCS models is principally non-gyrotropic. It was shown in numerical models of TCS [70], and later supported by experimental observations [71], that velocity distribution functions of ions in TCSs have non-isotropic, non-gyrotropic and non-Maxwellian pressure tensors. The characteristics of anisotropic pressure tensors in a self-consistent TCS model were investigated in detail in [72] and were in good agreement with earlier results [70]. Generally, because of the small thicknesses of TCSs and the corresponding violation of ion guiding center motion their description goes beyond the validity limits of MHD. In this paper we will mostly describe models using a kinetic description of particle dynamics as most adequate for TCS description.

Particle dynamics in the reversed magnetic field of a TCS is determined by the parameter adiabaticity, κ, which characterizes the ratio of the minimum curvature radius of the magnetic field line R_c to the maximum Larmor radius ρ_L near the neutral line: $\kappa = \sqrt{R_c/\rho_L}$. The parameter κ is the key parameter in particle dynamics. At $\kappa \gg 1$ plasma particles are fully magnetized and their motion can be described in a guiding center approximation. At $\kappa \sim 1$ particle motion becomes essentially nonlinear [73]. At $\kappa \ll 1$ particle gyroradii approximate the curvature radii of magnetic lines, and in this transitional regime particle motion becomes chaotic. For $\kappa < 1$ particle motion becomes quasi-adiabatic: the usual invariant magnetic moments are not conserved at this regime but the invariant of motion $I_z = (2\pi)^{-1}\oint p_z dz$ could be considered as being approximately conserved [66]. In this regime particles are still magnetized outside the CS but are demagnetized in the neutral plane and move along serpentine-like orbits, alternately crossing the CS moving from above and below. Within a TCS the X and Z degrees of freedom of serpentine motion are decoupled: particles perform fast vertical oscillations in the Z direction and simultaneous slow rotation in the XY plane. Near the separatrix separating two types of motion a small jump of integral of motion ΔI_z takes place so that $\Delta I_z \ll I_z$. It was shown that ΔI_z is proportional to the value of the parameter κ [16]. Together with Speiser particles having small values of invariant of motion I_z and moving along so-called transient trajectories, there also exist so-called quasi-trapped populations of particles that, contrary to Speiser's ones, go along quasi- closed orbits and can cross the CS many times; their I_z invariants are larger than for Speiser's particles [11]. Because the average square value of the jump ΔI_z is not equal to zero, CS crossing by quasi-trapped particles can be described as a diffusive process with a coefficient of diffusion $D = \langle(\Delta I_z)^2\rangle/T_{QT}$, where T_{QT} is the approximate time scale of the cycle of quasi-trapped particle motion. This process accompanied by the accumulation of quasi-trapped plasma, called 'CS aging' in [74]. In the magnetotail the electron parameter $\kappa_e \tilde{} 2 - 3$ while for ions this value is one order of magnitude smaller at $\kappa_i \tilde{} 0.1 - 0.2$. This

determines the principal difference in the dynamics of both particle species and the resulting peculiarities of the TCS itself. The motion of two plasma components can only be described in using a hybrid approach, when protons are described as quasi-adiabatic ones and electrons, for example, as an anisotropic conducting fluid.

An analytical self-consistent model of a TCS, taking into account both quasi-adiabatic protons and magnetized electrons, was first proposed in [49]. A TCS is so thin in comparison with scales in the X and Y directions that one can consider it as a 1D configuration, with all its characteristics depending only on the Z coordinate. Consider a simplified magnetic field $\boldsymbol{B} = \{B_x(z),0,B_n\}$, where the tangential component $B_x(z)$ reverses sign across the equatorial $z = 0$ plane (see figure 1). The normal component B_n is supposed to be constant. Thus particle flows come from the edges of the system (which corresponds in reality to a plasma mantle source) towards the neutral sheet plane ($z = 0$). The ion population is supposed to consist of transient and quasi-trapped particles with distribution functions, correspondingly, $f_{\text{trans}}(\vec{v}) \tilde{} \exp\{-[(v_\parallel - v_{\text{D}})^2 + v_\perp^2]/v_T^2\}\,\mathrm{d}\vec{v}$ and $f_{\text{trap}}(\vec{v}) \tilde{} \exp\{-v_0^2/v_{\text{T}}^2\}\,\mathrm{d}\vec{v}$ (v_{T} and v_{D} designate the thermal and bulk flow velocities, v_0 is the total speed). The ion population is described by the quasi-adiabatic approach so that the action integral of ion motion $I_z = (m/2\pi)\oint v_z \mathrm{d}z$ could be considered as approximately conserved. Electron dynamics is supposed to be fast enough to support a quasi-equilibrium Boltzmann distribution in the presence of an ambipolar electrostatic potential and mirror forces. Plasma quasi-neutrality $n_i \approx n_e$ is supported by these electrostatic fields. Such an approach generalizes earlier quasi-adiabatic model [75, 76] where electrostatic effects were not taken into account.

The model of a TCS is described by the self-consistent system of Vlasov–Maxwell equations:

$$\frac{\mathrm{d}B_x}{\mathrm{d}z} = (4\pi/c)(j_{yi}(z) + j_{ye}(z)), \tag{3}$$

where the ion current is the sum of currents carried by transient and trapped particles: $j_{yi} = (4\pi/c)\sum_i e\int v_y f_i(z,\vec{v})\mathrm{d}\vec{v}$. Here f_i is the local ith ion distribution function that can be extrapolated to the entire CS domain by its mapping from the edges of the TCS to the neutral plane using the quasi-adiabatic integral of motion I_z and applying the Liouville theorem. Finally, the generalized distribution functions of transient Speiser's and quasi-trapped particles acquire corresponding forms: $f_{\text{trans}}(\vec{v}) \tilde{} \exp\{-(\sqrt{v_0^2 - (\omega_0/m)I_z} - v_{\text{D}})^2 + (\omega_0/m)I_z/v_{\text{T}}^2\}$ and $f_{\text{trap}}(\vec{v}) \tilde{} \exp\{-v_0^2/v_{\text{T}}^2\}$. Taking into account the Boltzmann approximation for electrons, their transverse electron drift currents can be calculated in a guiding center approximation: $j_e = -en_e c[\vec{E} \times \vec{h}]/B + \frac{c}{B}[\vec{h} \times \vec{\nabla}_\perp p_{\perp e}] + \frac{c}{B}(p_{IIe} - p_{\perp e})[\vec{h} \times (\vec{h}\vec{\nabla})\vec{h}]$, where $\vec{h} = \vec{B}/B$. Expressions for the electron pressure can be found with the help of the Chou–Goldberger–Low approximation for the perpendicular direction and energy conservation for the parallel one.

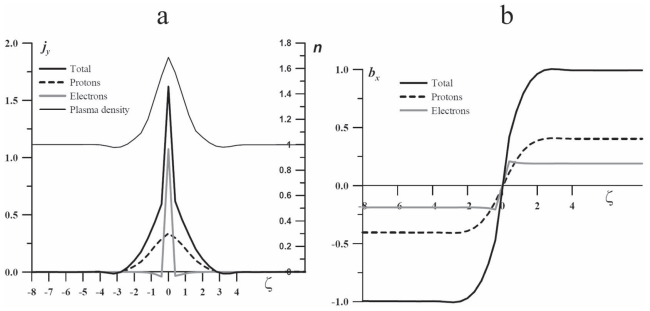

Figure 6. Self-consistent profiles of a TCS. In (a) one can see the total current and plasma densities (black thick and thin continuous lines, correspondingly) and the corresponding electron (gray continuous line) and ion (black dashed line) current densities in dimensionless variables: z coordinate $\zeta = z\omega_0/\varepsilon^{4/3}v_{\text{D}}$, current density $j_y(\zeta) = J_y\varepsilon^{-2/3}/(en_0v_{\text{D}})$.

Numerical solution of the Vlasov–Maxwell system of equations shown above demonstrates the multiscale character of a TCS, when a very narrow electron-dominated CS is embedded inside a significantly thicker proton-dominated CS [49]. Figure 6 shows the total current density, as well as separate electron and proton profiles (a), embedded inside a thicker plasma sheet (the profile of the plasma density $n(\zeta)$ is normalized to its value at the edges of the CS). Corresponding profiles of magnetic components are shown in figure 6(b).

If the plasma is a multicomponent one, particularly if it contains along with electrons and protons a population of a heavy ion (e.g.oxygen ions, typical for the post-substorm magnetotail), the profiles of current density and magnetic field acquire the additional scaling related to an additional CS with dominating oxygen populations.

The whole multiscale CS would be embedded inside the thickest plasma sheet [77].

Figure 6(b) shows the corresponding magnetic field profiles $b_x = B_x(z)/B_0$, where B_0 is the value of B_x at the edges of the CS, $\varepsilon = v_{\text{T}}/v_{\text{D}}$ is the parameter characterizing ion flow, v_{T} and v_{D} are, correspondingly, the thermal and flow velocities, and ω_0 is the proton gyrofrequency at the edges of the CS.

The temporal evolution of a TCS contaminated by scattered quasi-trapped plasma (the abovementioned TCS 'aging' process [74, 78]) is shown in figure 7. Due to peculiarities of quasi-trapped particle dynamics these particles support the local negative current in the CS center and a positive one at its edges. At the same time their net current is exactly zero because of the closeness of their orbits. The trapped particles can redistribute the current of transient Speiser particles that are the main current carriers in a TCS. Once the density of quasi-trapped particles becomes sufficiently large, the current density profile is transformed from a bell-like shape to a double-humped one.

The corresponding magnetic field profile demonstrates its flattening with the formation of a smoother profile near the neutral plane. Later these results were confirmed by observational data in the Earth's magnetotail [10, 79]. Thus, in [79]

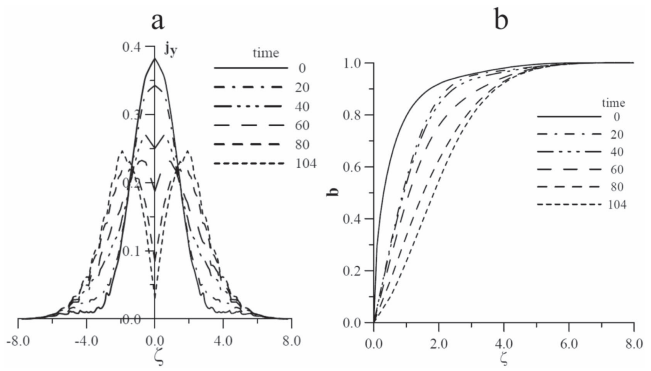

Figure 7. Snapshots of the temporal changing of TCS current density (a) (adapted from [78]) and magnetic field (b) during the 'aging' of the CS. The values of variables are dimensionless, as in figure 6.

several CS crossings by the Cluster spacecraft, with possible influence of a quasi-trapped plasma leading to the formation of smoothed and double-humped current density profiles from single-peaked as in figure 7(a), are demonstrated.

Therefore one can observe a large variety of CSs profiles in a space plasma. Electron drift currents [49], the presence of oxygen heavy ions [77] and the accumulation of quasi-trapped plasma in TCSs [74] represent realistic factors that influence the formation of complex multiscale profiles with several embedded CSs with different thicknesses in a different planetary magnetospheres [22, 46, 47]. Factors such as the shear magnetic component or the natural fluctuations of plasma sources can also lead to the formation of asymmetric TCS current density profiles [11, 50, 52, 80]. All these TCS configurations can have different structures and conditions of stability because they are mostly determined not by macroscopic characteristics of plasma flows but by the peculiar kinetic effects operating within the TCS.

6. Current sheet dynamics

Tearing (current filamentation) instability as the key factor in substorm activity of the Earth's magnetotail was proposed many years ago in [54], where the 1D Harris sheet equilibrium solution was used for stability analysis. Later, Schindler [81] showed that even a small normal component B_z in a CS can completely destroy the resonant Landau damping on electrons. The strong stabilizing effect of electrons magnetized by the small but finite normal component of the magnetic field means that tearing is no longer considered as a potential trigger of the onset of the expansion phase of substorms [81]. Neither stochastic motion [66] nor whistler pitch angle scattering were able to overcome the strong stabilizing effect of magnetized electron compressibility [56]. Ideas about possible tearing destabilization due to transient electrons and current-driven instabilities were elaborated later [53, ~~62~~]. Many other sophisticated possible routes to substorm activation were proposed to solve this problem [11, 13]. However, the main confusion in practically all earlier papers was related with the fact that all conclusions concerning the absence of tearing mode growth in CSs (see, e.g., [54, 56, 81, 82]) were based on the stability analysis of the Harris-like CS model. In both experimental observations [10, 50, 79] and in CS theory it was found that realistic CSs are principally different from Harris-like configurations. Also due to ~~PIC~~ modeling of collisionless reconnection (see [83]; Q4
reviews in [11, 13] and references therein) it was demonstrated that strong anisotropy of velocity distribution is characteristic for CSs, contrary to the isotropic Harris-like sheet. Therefore one needs to find the additional factors controlling the stability of a CS. The importance of distribution function anisotropy was investigated in papers about CS dynamics [58, 84, 85]. These results make the problem of analytical analysis of stability for anisotropic equilibria very real. Below we will demonstrate the results of this analysis where the principal elements of theoretical consideration in [81] were modified and adapted to a new 1D anisotropic TCS configuration.

The equation for the perturbation of the vector potential $A_{1y} \sim \exp(ikx - i\omega t)$ can be found from the energy principle in which the functional of the perturbed energy of tearing mode

$$W_{\text{tearing}} = \int_{-\infty}^{\infty} \left\{ |\nabla \times A_1|^2 + |\nabla \phi_1|^2 + \frac{4\pi}{c}\frac{\partial j_y}{\partial A_0}|A_1|^2 + 4\pi e \int_{-\infty}^{\infty} \frac{\tilde{f}_{1e}^2}{\partial \tilde{f}_{0e}/\partial \phi_0} \mathrm{d}\vec{v} \right\} \quad (4)$$

should be minimum, i.e.

$$\delta W_{\text{tearing}}(A_1)/\delta A_1 = 0. \quad (5)$$

This allows the determination of the boundary of marginal stability of a CS considered up to the second order of perturbation theory (as in [81]). The perturbed energy of the tearing mode contains three general terms: energies of perturbed magnetic and electric fields (first and second terms), free energy of configuration driving current filamentation $\sim \partial j_y/\partial A_0$ and a term describing the compressibility of electron fluids $\sim \tilde{f}_{1e}^2/\partial \tilde{f}_{0e}/\partial \phi_0$. Finally condition (5) can be reduced to a differential equation for the vector potential of perturbed magnetic field:

$$\frac{\mathrm{d}^2 A_1(z)}{\mathrm{d}z^2} - \left(k^2 + \frac{4\pi}{c}\frac{\partial j_y}{\partial A_0} + 4\pi \frac{n_{0e} T_e k^2}{B_z^2} \right) A_1(z) = 0. \quad (6)$$

Functional δW (4) was minimized for the wave number of perturbation k corresponding to a marginal stability condition $\delta W(A_{1y}) < 0$. The solutions $A_1(z)$ of equation (6) were found.

This allowed the parametric map of stable and unstable regions to be obtained. The tearing mode stability map for governing parameters ε and b_n is shown in figure 8(a). Unstable TCS domains where $\delta W < 0$ for at least one value of k are shaded black. As shown in this map the most unstable CSs have a strong anisotropic value $\varepsilon < 1$ and the optimal interval of parameter $b_n \tilde{} 0.1 - 0.2$.

This result has given the chance to revisit an old paradigm associating substorm activity with the onset of tearing-type instability. The idea that magnetotail CSs can become

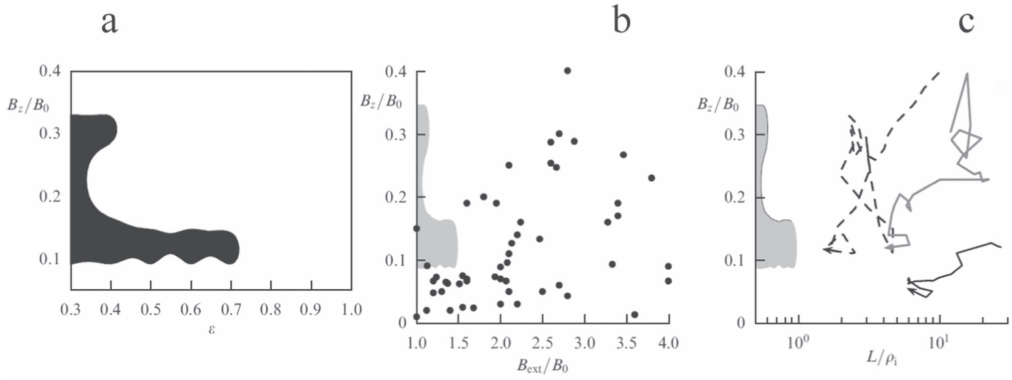

Figure 8. Parametric space of tearing stability of TCSs [13]. (a) A parametric map in the theory. Black shading shows the unstable region. (b) Map of the instability regions with the positions of the TCSs observed by Cluster. (c) A parametric instability map with the trajectories corresponding to CS evolution during the substorm growth phase.

unstable only in some narrow regions in a parameter space was formulated for the first time in [57]. In [62] this effect is revisited and investigated in detail in the framework of an adequate quasi-adiabatic model of TCS fully supported by modern '*in situ*' observations.

Therefore one can conclude that the thinning of a magnetotail CS is followed by increasing anisotropy of ion and electron distributions, and an initially isotropic and stable quite thick CS might be transformed into a new metastable equilibrium where the CS might experience topological changes enabling the process of fast reconnection [13, 86, 87]. Figure 8(b) demonstrates the parametric space corresponding to figure 8(c) where one can see characteristics of CSs observed by Cluster during substorms (see also [87]). Inside the gray regions the system is unstable and CSs will be destroyed. As a result we see a quite dense multitude of TCSs outside this region and a small number of TCSs inside this region. Figure 8(c) shows the hodograms of TCS states during substorms. Because of slow CS thinning, its parameters are changed. One can see that all hodograms are streaming from the right upper corner towards the instability region.

7. Conclusions

In this paper a short comparative analysis of planetary magnetospheres is given. It is shown that their self-organized formation in the SW is the result of the interaction of the internal planetary magnetic field with the incoming supersonic SW flow. As a result of this interaction, the planetary magnetospheres are usually compressed at the dayside and strongly elongated like a cometary tail at the nightside. It is interesting that even those planets without an intrinsic magnetic field also form a kind of magnetosphere due to the induced currents flowing in the ionosphere and supporting the current system forming the tail-like structure. Finally, depending on the value of the planetary magnetic field (including planets without any magnetic field), these magnetospheres form a more or less complex internal structure.

Thin current structures are observed in magnetospheres practically everywhere (on magnetopauses, shock waves, in the tails) and play an important role as reservoirs of free magnetic energy necessary for the beginning of magnetic reconnection. The TCS hybrid model [49] based on quasi-adiabatic proton dynamics has been successful in the interpretation of observational data and in predicting TCS properties: multiscale structure, embedding and metastability. It becomes possible to solve the long-standing theoretical paradigm of magnetotail stability during substorms and explain TCS metastability, i.e. the ability of a TCS to remain in a stable state for a long time, and then spontaneously change magnetic topology and initiate fast plasma acceleration and heating Thus, it is shown that TCSs are universal structures in the collisionless space plasma and they are necessary mediators of energy exchange between the SW and planetary magnetospheres.

Acknowledgments

The authors are grateful to A Artemyev for useful discussions. The work of L Zelenyi and E Grigorenko was supported by RSF (grant no. 16-42-01103). The work of HM was made in a frame of RFBR grant 17-02-01328, program PRAN I.24II and Volkswagen grant AZ90 312/contract 1344. The work of VP was supported by the program 28 PRAN, Program 'PLASMA' and RFBR grant 16-52-16009 NCNIL.

ORCID iDs

Helmi Malova https://orcid.org/0000-0001-6511-2335

References

Q5

[1] Biermann L and Schluter A 1951 *Phys. Rev.* **82** 863
[2] Parker E N 1958 *Phys. Fluids* **1** 171
[3] Gold T 1959 *J. Geophys. Res.* **64** 1665
[4] Gringauz K, Bezrokikh V, Ozerov V and Rybchinskii R 1960 *Sov. Phys. Dokl.* **5** 361
[5] Ness N 1965 *J. Geophys. Res.* **70** 2989

[6] Alexeev I, Belenkaya E, Kalegaev V, Feldstein Y and Grafe A 1996 *J. Geophys. Res.* **101** 7737
[7] Sergeev V, Mitchell D, Russell C and Williams D 1993 *J. Geophys. Res.* **98** 17345
[8] McPherron R, Nishida A and Russell C 1987 *Quantitative Modeling of Magnetosphere-Ionosphere Coupling Processes* (Kyoto, Japan) p 252
[9] Baker D, Pulkinen T, Angelopoulos V, Baumjohann W and McPherron R 1996 *J. Geophys. Res.* **101** 12975
[10] Runov A *et al* 2005 *Ann. Geo.* **23** 1
[11] Zelenyi L, Malova K H, Artemyev A, Popov V and Petrukovich A 2011 *Plasma Phys. Rep.* **37** 118
[12] Lui A, Lopez R, Anderson B, Takahashi K, Zanetti L, McEntire R, Potemra T, Klumpar D, Greene E and Strangeway R 1992 *J. Geophys. Res.* **97** 1461
[13] Zelenyi L, Artemyev A, Malova K H, Petrukovich A and Nakamura R 2010 *Phys.-Usp.* **53** 933
[14] Malova H, Popov V, Grigorenko E, Petrukovich A, Delcourt D, Sharma A, Khabarova O and Zelenyi L 2017 Q6 *Astrophys. J.* **834** 1
[15] Zelenyi L, Oka M, Malova H, Fujimoto M, Delcourt D and Baumjohann W 2007 *Space Sci. Rev.* **132** 593
[16] Zelenyi L, Malova H, Grigorenko E and Popov V 2016 *Phys.-Usp.* **186** 1057
[17] Syrovatskii S 1971 *Sov. J. Exp. Theor. Phys.* **33** 933
[18] Frank A, Kyrie N, Markov V and Voronova E 2018 *Plasma Phys. Rep.* **44** 551
[19] ~~Kivelson M and Bagenal F 2007 *Encyclopedia of the Solar System* 519~~ Q7
[20] Siscoe G 1975 *Icarus* **24** 311
[21] Voight G-H, Hill T and Dessler A 1983 *Astrophys. J.* **266** 390
[22] Vasko I, Malova H, Artemyev A and Zelenyi L 2012 *Planet. Space Sci.* **96** 81
[23] Khurana K, Kivelson M, Vasyliunas V, Krupp N, Woch J, Lagg A, Mauk B and Kurth W 2004 *Jupiter. The Planet, Satellites and Magnetosphere* vol 1 (Cambridge, UK: Cambridge University Press) p 593
[24] Bagenal F 1991 *Bull. Amer. Astron. Soc.* **23** 1152
[25] Zimbardo G 1989 *J. Geophys. Res.* **94** 8707
[26] Kislov R, Malova K H and Vas'ko I 2013 *Moscow Univers. Phys. Bull.* **68** 82
[27] Axford W, Petschek H and Siscoe G 1965 *J. Geophys. Res.* **70** 1231
[28] Panov E, Buchner J, Franz M, Korth A, Savin S, Reme H and Fornacon K-H 2008 *J. Geophys. Res.* **113** A01220
[29] Sibeck D, Lopez R and Roelof E 1991 *J. Geophys. Res.* **96** 5489
[30] Nagata T 1963 *Planet. Space Sci.* **11** 1395
[31] Bame S, Asbridge J, Felthauser H, Hones E and Strong I 1967 *J. Geophys. Res.* **72** 113
[32] Siscoe G and Kaymaz Z 1999 *J. Geophys. Res.* **104** 14639
[33] Chapman S and Ferraro V 1931 *Terrest. Magn. Atmos. Elec.* **36** 171
[34] Ogilvie K, Scudder J, Vasyliunas V, Hartle R and Siscoe G 1977 *J. Geophys. Res.* **82** 1807
[35] Bagenal F 2001 Planetary magnetospheres *Encyclopedia of Astronomy and Astrophysics* (Bristol, UK: Institute of Physics Publishing) 1
[36] Fujimoto M, Baumjohann W, Kabin K, Nakamura R, Slavin J, Terada N and Zelenyi L 2007 *Space Sci. Rev.* **132** 529
[37] Anderson B *et al* 2010 *Space Sci. Rev* **152** 307
[38] Zelenyi L and Vaisberg O 1982 *Cosmic Res.* **20** 604
[39] Luhmann J, Elphic R, Russell C, Slavin J and Mihalov J 1981 *Geophys. Res. Lett.* **8** 517
[40] Vennerstrom S 2011 *Icarus* **215** 234
[41] Dubinin E, Fraenz M, Woch J, Barabash S and Lundin R 2009 *Geophys. Res. Lett.* **36** L08108
[42] Vaisberg O and Zeleny L 1984 *Icarus* **58** 412
[43] Volwerk M, Delva M, Futaana Y, Retino A, Voros Z, Zhang T, Baumjohann W and Barabash S 2009 *Ann. Geophys.* **27** 2321–30
[44] Russell C, Kivelson M, Khurana K and Huddleston D 2000 *Adv. Space Res.* **26** 1671
[45] Vasyliunas V 1975 The magnetospheres of the Earth and Jupiter *Proc. Neil Brice Memor. Symp. (Frascati, Italy, 28 May–1 June 1974)* p 179
[46] Grigorenko E, Shuvalov S, Malova H, Dubinin E, Popov V and Zelenyi L 2017 *J. Geophys. Res.* **122** 1
[47] Vasko I, Zelenyi L, Artemyev A, Petrukovich A, Malova H, Zhang T, Fedorov A, Popov V, Barabash S and Nakamura R 2014 *Planet. Space Sci.* **96** 81
[48] Whang Y 1977 *J. Geophys. Res.* **82** 1024
[49] Zelenyi L, Malova H, Popov V, Delcourt D and Sharma A 2004 *Nonlin. Proc. Geophys.* **11** 579
[50] Runov A *et al* 2006 *Ann. Geophys.* **24** 247
[51] Asano Y, Nakamura R, Baumjohann W, Runov A, Voros Z, Volwerk M, Zhang T, Balogh A, Klecker B and Reme H 2005 *Geophys. Res. Lett.* **32** L03108
[52] Malova H *et al* 2015 *J. Geophys. Res.* **120** 1
[53] Zelenyi L, Malova H, Artemyev A, Popov V, Petrukovich A, Delcourt D and Bykov A 2009 *Climate and Weather of the Sun–Earth System (CAWSES)* (Tokyo: Terrapub) p 121
[54] Coppi B, Laval G and Pellat R 1966 *Phys. Rev. Lett.* **16** 1207
[55] Harris E 1962 *Nuovo Cim.* **23** 115
[56] Pellat R, Coroniti F and Pritchett P 1991 *Geophys. Res. Lett.* **18** 143
[57] Galeev A and Zelenyi L 1976 *Transl. Zhurn. Eksperim. Teor. Fiz.* **70** 2133
[58] Karimabadi H, Daughton W, Pritchett P and Krauss-Varban D 2003 *J. Geophys. Res.* **108** 1400
[59] Buchner J and Kuska J-P 1999 *Ann. Geophys.* **17** 604
[60] Voronkov I, Rankin R, Frycz P, Tikhonchuk V and Samson J 1997 *J. Geophys. Res.* **102** 9639
[~~61~~] Speiser T 1965 *J. Geophys. Res.* **70** 4219 Q8
[~~62~~] Zelenyi L, Artemyev A, Malova H and Popov V 2008 *J. Atmos. Solar Terr. Phys.* **70** 325
[~~63~~] Zelenyi L, Artemyev A, Petrukovich A, Nakamura R, Malova H and Popov V 2009 *Ann. Geophys.* **27** 861
[~~64~~] Birn J, Sommer R and Schindler K 1975 *Astrophys. Space Sci.* **35** 389
[~~65~~] Cheng C 1992 *J. Geophys. Res.* **97** 1497
[66] Buchner J and Zelenyi L 1989 *J. Geophys. Res.* **94** 11821
[67] Eastwood J 1972 *Planet. Space Sci.* **20** 1555
[68] Kropotkin A and Domrin V 1996 *J. Geophys. Res.* **101** 19893
[69] Ashour-Abdalla M, Berchem J, Buchner J and Zelenyi L 1991 *Geophys. Res. Lett.* **18** 1603
[70] Ashour-Abdalla M, Zelenyi L, Peroomian V and Richard K 1994 *J. Geophys. Res.* **99** 14891
[71] Artemyev A, Petrukovich A, Nakamura R and Zelenyi L 2010 *J. Geophys. Res.* **115** A12255
[72] Mingalev O, Mingalev I, Malova K H and Zelenyi L 2007 *Plasma Phys. Rep.* **33** 942
[73] Delcourt D, Malova H and Zelenyi L 2004 *J. Geophys. Res.* **109** A01222
[74] Zelenyi L, Delcourt D, Malova H and Sharma A 2002 *Geophys. Res. Lett.* **29** 49–1
[75] Sitnov M, Zelenyi L, Malova H and Sharma A 2000 *J. Geophys. Res.* **105** 13029
[76] Zelenyi L, Sitnov M, Malova H and Sharma A 2000 *Nonlin. Proc. Geophys.* **7** 127
[77] Zelenyi L, Malova H, Popov V, Delcourt V, Ganushkina N and Sharma A 2006 *Geophys. Res. Lett.* **33** L05105
[78] Zelenyi L, Malova H and Popov V 2003 *JETP Lett.* **78** 296
[79] Nakamura R, Baumjohann W, Runov A and Asano Y 2006 *Space Sci. Rev.* **122** 29
[80] Malova H, Zelenyi L, Popov V, Delcourt D, Petrukovich A and Runov A 2007 *Geophys. Res. Lett.* **34** L16108

[81] Schindler K 1979 *Space Sci. Rev.* **23** 365
[82] Lembege B and Pellat R 1982 *Phys. Fluids* **25** 1995
[83] Pritchett P 2005 *J. Geophys. Res.* **110** A10213
[84] Daughton W 2002 *Phys. Plasmas* **9** 3668
[85] Sitnov M, Swisdak M, Drake J, Guzdar P and Rogers B 2004 *Geophys. Res. Lett.* **31** L09805
[86] Birn J, Hesse M and Schindler K 2006 *Space Sci. Rev.* **124** 103
[87] Zelenyi L, Kropotkin A, Domrin V, Artemyev A, Malova H and Popov V 2009 *Cosmic Res.* **47** 352